BIOCHEMISTRY
including biophysical chemistry & molecular biology

Article

pubs.acs.org/biochemistry

Crystal Structure of *Pedobacter heparinus* Heparin Lyase Hep III with the Active Site in a Deep Cleft

Wataru Hashimoto,*[,†] Yukie Maruyama,[†] Yusuke Nakamichi,[†] Bunzo Mikami,[‡] and Kousaku Murata[†,§]

[†]Laboratory of Basic and Applied Molecular Biotechnology, Graduate School of Agriculture, Kyoto University, Uji, Kyoto 611-0011, Japan

[‡]Laboratory of Applied Structural Biology, Graduate School of Agriculture, Kyoto University, Uji, Kyoto 611-0011, Japan

Supporting Information

ABSTRACT: *Pedobacter heparinus* (formerly known as *Flavobacterium heparinum*) is a typical glycosaminoglycan-degrading bacterium that produces three heparin lyases, Hep I, Hep II, and Hep III, which act on heparins with 1,4-glycoside bonds between uronate and amino sugar residues. Being different from Hep I and Hep II, Hep III is specific for heparan sulfate. Here we describe the crystal structure of Hep III with the active site located in a deep cleft. The X-ray crystallographic structure of Hep III was determined at 2.20 Å resolution using single-wavelength anomalous diffraction. This enzyme comprised an N-terminal α/α-barrel domain and a C-terminal antiparallel β-sheet domain as its basic scaffold. Overall structures of Hep II and Hep III were similar, although Hep III exhibited an open form compared with the closed form of Hep II. Superimposition of Hep III and heparin tetrasaccharide-bound Hep II suggested that an active site of Hep III was located in the deep cleft at the interface between its two domains. Three mutants (N240A, Y294F, and H424A) with mutations at the active site had significantly reduced enzyme activity. This is the first report of the structure−function relationship of *P. heparinus* Hep III.

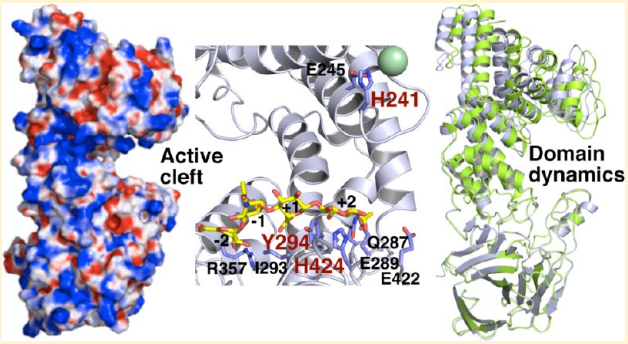

Glycosaminoglycans are widely distributed in mammals as components of extracellular matrices and are involved in cell−cell associations, cell signaling, and cell growth and differentiation.[1] These polysaccharides are composed of repeating disaccharide units each consisting of a uronic acid residue (glucuronic or iduronic acid) and an amino sugar residue (glucosamine or galactosamine); these constituent monosaccharides are often sulfated.[2] Because of their variety of sugar compositions, modes of glycoside bonds, acetylation, and sulfation, glycosaminoglycans are classified into several groups, including chondroitin, dermatan sulfate, hyaluronan, heparin, and heparan sulfate.[3]

Chondroitin consists of D-glucuronic acid (GlcUA) and *N*-acetyl-D-galactosamine (GalNAc) with a sulfate group(s) at position 4 or 6 or both. Hyaluronan consists of GlcUA and *N*-acetyl-D-glucosamine (GlcNAc). Being distinct from chondroitin, dermatan sulfate, and hyaluronan with 1,3-glycoside bonds between uronic acid and amino sugar residues, heparin and heparan sulfate contain 1,4-glycoside bonds. The differences between heparin and heparan sulfate are in their L-iduronic acid (IdoA) and sulfate group contents, with heparin having more IdoA and sulfate groups.

Degradation of glycosaminoglycans by bacteria has been investigated to clarify bacterial infection mechanisms and to determine the complex structures of mucopolysaccharides.[4,5] *Streptococcus pneumoniae* produces hyaluronate lyase as a spreading factor for degradation of hyaluronans in the extracellular matrices of mammals.[6] *Pedobacter heparinus* (formerly *Flavobacterium heparinum*) isolated from soil has been extensively investigated as a heparin-degrading bacterium.[7,8] This bacterium produces three heparin lyases as wells as two chondroitinases, which are different in terms of their sequence similarity and substrate specificity.[9] On the basis of their primary structures, polysaccharide lyases are classified into 22 families (PL-1−PL-22).[10] Family PL-6 chondroitinase B adopts the right-handed parallel β-helix fold as a basic scaffold,[11] while family PL-8 chondroitinase AC comprises N-terminal α/α-barrel and C-terminal antiparallel β-sheet domains.[12] Family PL-13 heparin lyase I (Hep I) prefers heparin with high degrees of sulfation, whereas family PL-12 heparin lyase III (Hep III) is specific for heparan sulfate, which includes sulfate group-free GlcUA-GlcNAc as a major disaccharide repeating unit[1] (Figure 1a). Thus, Hep III is termed heparan sulfate lyase. On the other hand, family PL-21 heparin lyase II (Hep II) is active on both heparin and heparan sulfate.

On the basis of their biochemical and biophysical significance, *Pedobacter* Hep I, Hep II, and Hep III have been

Received: September 9, 2013
Revised: January 15, 2014
Published: January 17, 2014

   dx.doi.org/10.1021/bi4012463 | *Biochemistry* 2014, 53, 777−786

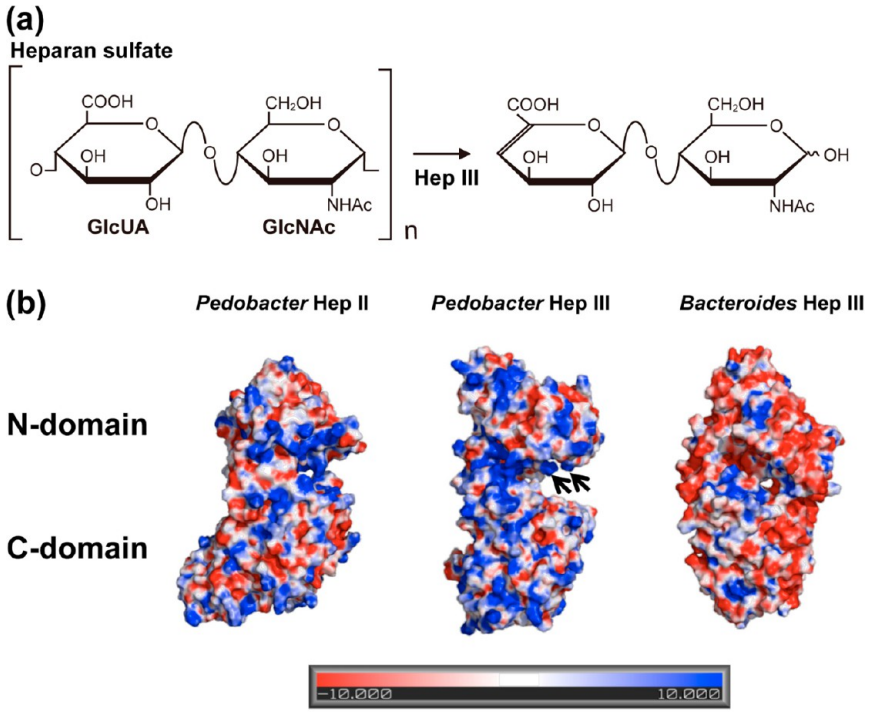

Figure 1. Heparin lyases. (a) Scheme for the degradation of heparan sulfate by Hep III. Heparan sulfate includes sulfate group-free GlcUA-GlcNAc as a major disaccharide repeating unit.[1] (b) Electrostatic features on the molecular surface model: (left) *Pedobacter* Hep II, (center) *Pedobacter* Hep III, and (right) *Bacteroides* Hep III. Positive and negative charges are colored blue and red, respectively. Positively charged clusters at the active cleft of *Pedobacter* Hep III are denoted with arrows.

thoroughly investigated by enzymology and site-directed mutagenesis.[13−19] For example, each of 13 histidine residues of *Pedobacter* Hep III (His-36, His-105, His-110, His-139, His-152, His-225, His-234, His-241, His-295, His-424, His-469, His-510, and His-539) has been substituted with an Ala residue, and subsequently, His-295 and His-510 have been demonstrated to be crucial for Hep III activity.[20] The structure−function relationships of family PL-13 *Bacteroides thetaiotaomicron* Hep I and family PL-21 *Pedobacter* Hep II have also been studied by X-ray crystallography.[21,22] No crystal structure of family PL-12 heparan sulfate lyase has been reported to date, although a heparinase III from *B. thetaiotaomicron* was recently analyzed structurally.[23] The level of sequence identity between *Pedobacter* and *Bacteroides* Hep IIIs is only 28%, although both are categorized into family PL-12. A significant difference in the isoelectric point between both is observed (*Pedobacter* Hep III, theoretical pI of 9.0; *Bacteroides* Hep III, theoretical pI of 4.9) (Figure 1b). There are no experimental data for structure-based functional analysis of amino acid residues that are crucial for Hep III enzymatic activity.

In this report, we describe the structure−function relationship of *P. heparinus* heparan sulfate lyase (Hep III) by X-ray crystallography, site-directed mutagenesis, and differential scanning fluorimetry.

MATERIALS AND METHODS

Molecular Cloning. An expression system for the signal peptide-truncated *Pedobacter* Hep III (ORF ID in the bacterial genome database, Phep_3797) from *P. heparinus* NBRC 12017 (DSM 2366) purchased from the NBRC collection was constructed in *Escherichia coli* cells as follows. To introduce the *Pedobacter* Hep III gene into a pET21b expression vector (Novagen), polymerase chain reactions (PCRs) were run using KOD-Plus polymerase (Toyobo), the genomic DNA of *P. heparinus* as a template, and two synthetic oligonucleotides (Hokkaido System Science) as primers. The sequences of oligonucleotides with *Nde*I and *Xho*I sites added to their 5′ regions for *Pedobacter* Hep III are listed in Table S1 of the Supporting Information. The pET21b vector was designed to express proteins with a hexahistidine (His_6)-tagged sequence at the C-terminus. The amplified truncated gene fragment was digested with *Nde*I and *Xho*I and then ligated with *Nde*I- and *Xho*I-digested pET21b. The resulting plasmid containing the truncated gene was designated pET21b-Phep_3797. In addition to the wild-type gene for *Pedobacter* Hep III, a mutant gene for the double mutant (I29V/L657S) of *Pedobacter* Hep III was unexpectedly amplified through the PCR procedure.

Protein Expression and Purification. *E. coli* strain BL21(DE3) or B834(DE3) (Novagen) was used as a host for *Pedobacter* Hep III expression. For expression in *E. coli*, cells were aerobically precultured at 30 °C in Luria-Bertani (LB) medium[24] supplemented with sodium ampicillin (0.1 mg/mL). For expression of a *Pedobacter* Hep III derivative with selenomethionine, *E. coli* cells were aerobically cultured in a minimal medium[25] supplemented with 25 μg/mL selenomethionine. When the culture turbidity was approximately 0.5 at 600 nm, isopropyl β-D-thiogalactopyranoside was added to the culture (0.1 mM) and the cells were cultured at 16 °C for an additional 44 h. Unless otherwise specified, all purification procedures were conducted at 0−4 °C. Recombinant *Pedobacter* Hep III was purified from *E. coli* cells harboring pET21b-Phep_3797 to homogeneity through cell disruption by sonication followed using column chromatography with three different separation media, affinity [TALON (Clonetech, 1.0 cm × 10 cm)], cation-exchange [Toyopearl CM-650M (Tosoh, 2.6 cm × 9.5 cm)], and gel filtration [Sephacryl S-200HR (GE

dx.doi.org/10.1021/bi4012463 | *Biochemistry* 2014, 53, 777−786

Table 1. Data Collection and Refinement Statistics

	Pedobacter Hep III wild type	*Pedobacter* Hep III with selenomethionine	I29V/L657S
	Data Collection[a]		
wavelength (Å)	1.0000	0.9790	1.0000
space group	$P2_12_12_1$	$P2_12_12_1$	$P2_12_12_1$
cell dimensions			
a (Å)	41.2	42.7	44.7
b (Å)	104.1	105.4	102.9
c (Å)	143.3	145.8	149.2
resolution limit (Å)	50.00−2.20 (2.28−2.20)	50.00−2.70 (2.80−2.70)	50.00−2.40 (2.49−2.40)
no. of measured reflections	257911	149613	210361
no. of unique reflections	32238	18682	27715
redundancy	8.0 (8.1)	8.0 (8.1)	7.6 (7.3)
completeness (%)	99.9 (100)	100 (100)	99.7 (99.5)
$I/\sigma(I)$	34.5 (6.8)	26.7 (6.2)	38.3 (4.1)
R_{merge}	0.108 (0.424)	0.131 (0.496)	0.078 (0.398)
	Refinement		
R_{cryst}	0.195		0.205
R_{free}	0.244		0.249
no. of molecules per asymmetric unit	1		1
no. of non-hydrogen atoms			
proteins	5214		5201
calcium ions	2		2
water molecules	131		61
average *B* factor (Å^2)	31.9		58.7
rmsd from ideal			
bond lengths (Å)	0.005		0.006
bond angles (deg)	0.995		1.079
Ramachandran plot (%)			
most favored regions	98.0		98.1
allowed regions	2.0		1.9

[a]Data from the highest-resolution shells are given in parentheses.

Healthcare, 2.6 cm × 65 cm)]. Protein purity was confirmed using sodium dodecyl sulfate−polyacrylamide gel electrophoresis (SDS−PAGE).[26] Protein contents were determined by measuring the absorbance at 280 nm using a 1 cm path length cuvette and assuming that E_{280} = 1.75 (*Pedobacter* Hep III) corresponded to 1 mg/mL.

Enzyme Assay. The enzyme was incubated in a 0.5 mL reaction mixture containing 0.01% substrate [heparan sulfate (Iduron), sodium heparin, chondroitin A, chondroitin C (Nacalai Tesque), or hyaluronan (Fluka)] and 50 mM Tris-HCl (pH 7.5). The activity was determined by monitoring the increase in absorbance at 235 nm. One unit of enzyme activity was defined as the amount of enzyme required to produce an increase of 1.0/min in absorbance at 235 nm.

Crystallization and X-ray Diffraction. For crystallization, purified native and selenomethionine derivative forms of *Pedobacter* Hep III were concentrated to ∼5 mg/mL by ultrafiltration with a Centriprep (Millipore). *Pedobacter* Hep III was crystallized at 20 °C using the sitting-drop vapor-diffusion method. The crystallization conditions were initially screened by sparse-matrix screening, which was conducted in a 96-well Intelli-plate (Art Robbins instruments) by using commercial crystallization kits purchased from Hampton Research, Jena Science, and Emerald Biosystems. A mixture (50 μL) of 20% polyethylene glycol 3000, 0.2 M calcium acetate, and 0.1 M Tris-HCl (pH 7.0) was used as a reservoir solution, and *Pedobacter* Hep III (1 μL) was mixed with this reservoir solution (1 μL) to form a drop. Another reservoir solution [20% polyethylene glycol 3350, 0.2 M sodium acetate, and 0.1 M Bis-Tris propane (pH 7.5)] was also suitable for crystallization of *Pedobacter* Hep III. For cryoprotection, a protein crystal was soaked in the reservoir solution containing 20% glycerol. A crystal was picked up from the soaking solution with a mounted nylon loop (Hampton Research) and placed directly into a cold nitrogen gas stream at −173 °C. For phasing, the derivative crystal with selenomethionine was prepared in a manner similar to that used for the native crystal. X-ray diffraction images were acquired for the native and derivative crystals at −173 °C under a nitrogen gas stream with a Quantum 315 CCD detector (ADSC) and synchrotron radiation (λ of 1 Å for the native crystal or 0.9790 Å for the derivative crystal) at the BL-38B1 station of SPring-8. Diffraction data were processed using the *HKL2000* program package.[27] Data collection statistics for native and derivative crystals are listed in Table 1.

Structure Determination and Refinement. The crystal structure of *Pedobacter* Hep III was resolved using single-wavelength anomalous diffraction with the selenomethionine derivative crystal. Phase determination and initial model building for the *Pedobacter* Hep III derivative were conducted using *PHENIX*.[28] *COOT*[29] was used to manually modify the initial model. Initial rigid body refinement and several rounds of restrained refinement against the data set were conducted using *REFMAC5*.[30] Water molecules were incorporated where the difference in density exceeded 3.0 σ above the mean, and the $2F_o - F_c$ map showed a density of >1.2 σ. Refinement continued until convergence was reached at 2.20 Å resolution. The final model quality was checked with *RAMPAGE*.[31] Figures

dx.doi.org/10.1021/bi4012463 | *Biochemistry* 2014, 53, 777−786

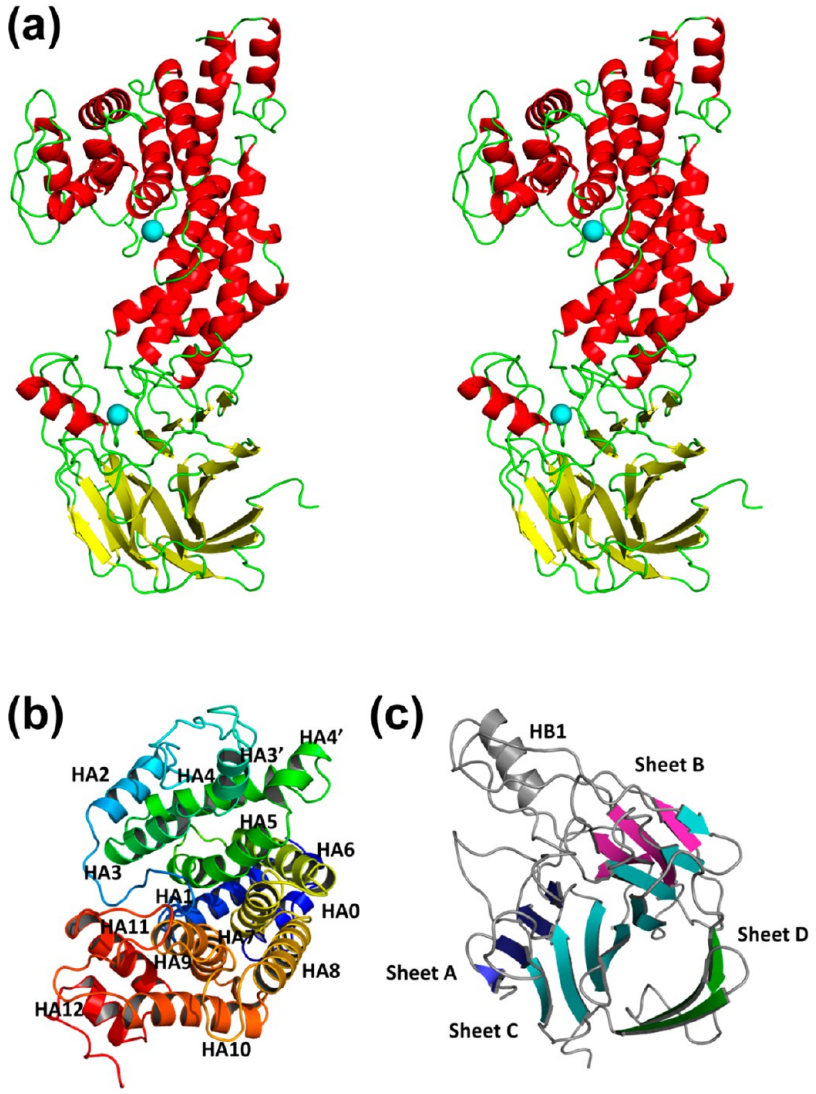

Figure 2. Structure of *Pedobacter* Hep III. (a) Overall structure (stereodiagram) (calcium ion shown as the cyan sphere). Colors denote secondary structure elements (red for α-helices, yellow for β-strands, and green for loops and coils). (b) N-Terminal α/α-barrel composed of 12 α-helices. (c) C-Terminal antiparallel β-sheets (sheets A–D).

for ribbon plots and surface models were prepared using *PyMOL*.[32] Coordinates used in this report were obtained from the Protein Data Bank (PDB), Research Collaboratory for Structural Bioinformatics, Rutgers University, New Brunswick, NJ (http://www.rcsb.org/).[33]

Site-Directed Mutagenesis. To substitute Glu-237, Gln-238, Asn-240, His-241, Tyr-294, Trp-350, Phe-423, His-424, Tyr-450, and Tyr-590 of *Pedobacter* Hep III with Ala, Ala, Ala, Ala, Phe, Ala, Ala, Ala, Phe, and Phe, respectively, 20 oligonucleotides were synthesized at Hokkaido System Science as described in Table S1 of the Supporting Information. Site-directed mutagenesis was performed using plasmid pET21b-Phep_3797 as a template and synthetic oligonucleotides as sense and antisense primers using the methods described in a QuickChange site-directed mutagenesis kit (Stratagene), except KOD-Plus polymerase was used for PCR. The resulting plasmids with mutations were used for mutant expression. Mutations were confirmed using DNA sequencing.[34] *E. coli* host strain cells were transformed using each plasmid.

Differential Scanning Fluorimetry. Interactions between *Pedobacter* Hep III and various saccharides were analyzed using differential scanning fluorimetry as described by Niesen et al.[35] using a MyiQ2 real-time PCR instrument (Bio-Rad). Heparin di- and tetrasaccharides (Iduron), gellan tetrasaccharide (unsaturated glucuronyl-glucosyl-rhamnosyl-glucose),[36] and GlcNAc were used as ligand saccharides. Fluorescence derived from a commercial dye, SYPRO Orange (Invitrogen), was monitored using filters provided with the PCR instrument (excitation at 492 nm and emission at 610 nm). A reaction mixture (20 μL) that included *Pedobacter* Hep III (0.232 mg/mL = 3.1 μM), each saccharide (0–1.0 mM), SYPRO Orange (1000-fold dilution), and Tris-HCl (20 mM, pH 7.5) was subjected to heat treatment. The temperature was increased from 25 to 95 °C at a rate of 0.5 °C/cycle (10 s/cycle) for a total of 141 cycles. The fluorescence emitted from SYPRO Orange after it bound to a denatured protein was measured. The fluorescence profile was obtained by plotting the relative fluorescence unit (RFU) at each temperature. The resulting fluorescence profile was analyzed using *iQ5* (Bio-Rad), and the midpoint of the increase in the profile was defined as the melting temperature.

dx.doi.org/10.1021/bi4012463 | *Biochemistry* 2014, 53, 777–786

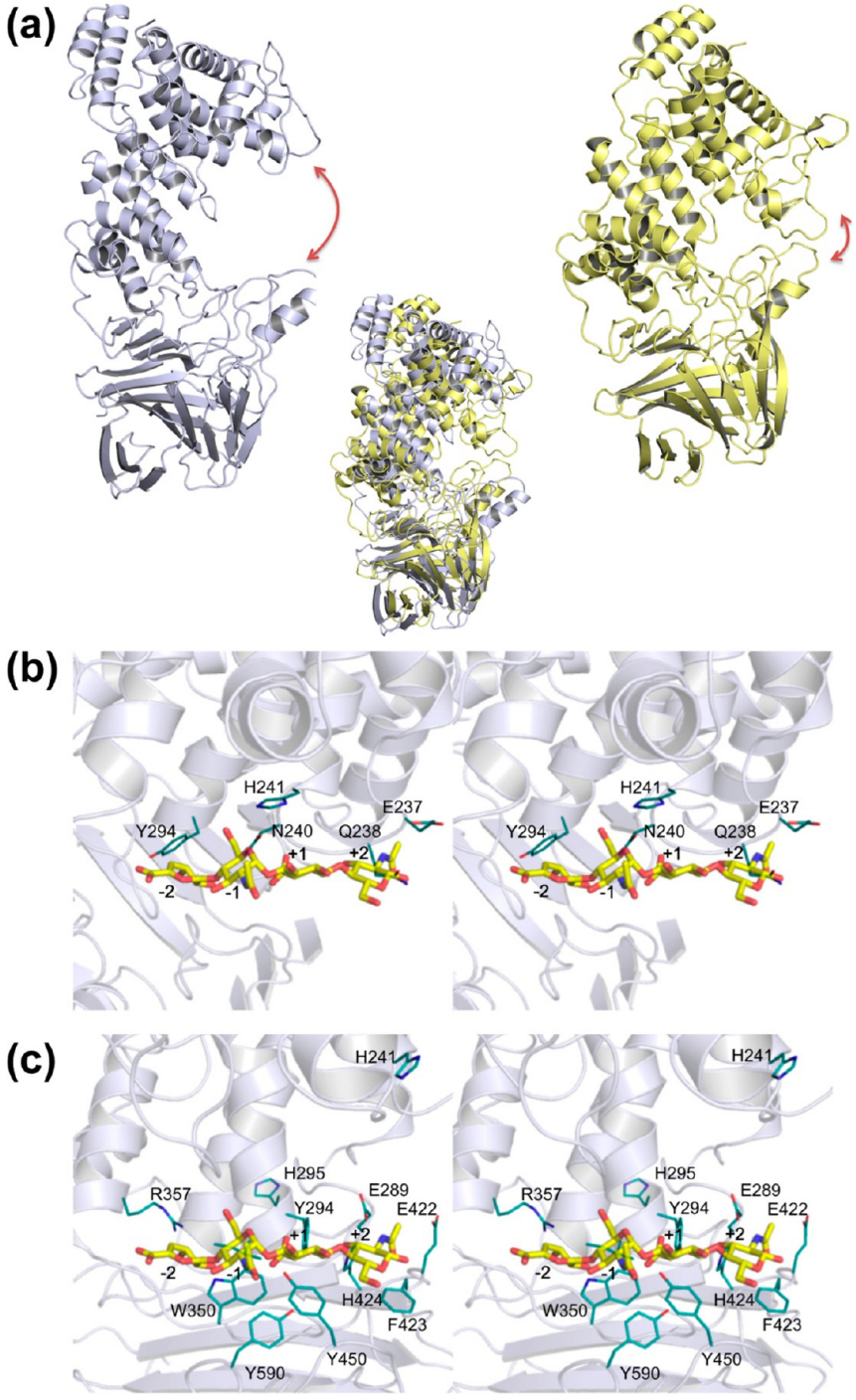

Figure 3. Structural comparisons. (a) Superimposition of *Pedobacter* Hep III (steel blue) and *Bacteroides* Hep III (yellow). (b) Superimposition of the N-terminal domains of *Pedobacter* Hep III and *Pedobacter* Hep II/tetrasaccahride (stereodiagram). (c) Superimposition of the C-terminal domain of *Pedobacter* Hep III and the central subdomain of *Pedobacter* Hep II/tetrasaccahride (stereodiagram). The tetrasaccharide (ΔGlcUA-GlcNAc-GlcUA-GlcNAc) from coordinates of *Pedobacter* Hep II/tetrasaccahride (PDB entry 3e7j) is colored yellow (carbon atom), red (oxygen atom), and blue (nitrogen atom). Probable residues of *Pedobacter* Hep III crucial for binding the tetrasaccharide are colored cyan (carbon atom), red (oxygen atom), and blue (nitrogen atom).

Accession Number. The atomic coordinates and structure factors of *Pedobacter* Hep III (entry 4mmh) and its I29V/L657S mutant (entry 4mmi) were deposited in the PDB.

RESULTS AND DISCUSSION

Crystallization and Structure Determination. *Pedobacter* Hep III (ORF ID, Phep_3797) consists of 659 residues with a signal peptide of 24 residues (Met-1−Ala-24). The recombinant *Pedobacter* Hep III protein expressed in *E. coli* cells did not include the signal peptide (Thr-2−Ala-24) but did include eight additional residues (Leu-Glu-His-His-His-His-His-His) at its C-terminus. This indicated that the recombinant enzyme contained 644 residues with an N-terminal sequence of Met-1-Gln-25-Ser-26-Ser-27 and a C-terminal sequence of Leu-657-Val-658-Pro-659-Leu-660-Glu-661-His-662-His-663-His-664-His-665-His-666-His-667. The recombinant *E. coli* cells

dx.doi.org/10.1021/bi4012463 | *Biochemistry* 2014, 53, 777−786

produced significant amounts of the enzyme in a soluble form, and purified *Pedobacter* Hep III (19.4 mg) was obtained from 4.5 L of LB culture (Figure S1a of the Supporting Information). Similar to the native enzyme from *P. heparinus*,[9] the recombinant enzyme was specific for heparan sulfate (specific activities of 22.6 ± 2.90 units/mg for heparan sulfate and 1.11 ± 0.157 units/mg for sodium heparin). Thus, to analyze its three-dimensional structure, the recombinant enzyme was subjected to crystallization.

Two different stick-shaped crystals of *Pedobacter* Hep III were found under different crystallization conditions. One was in droplet A comprising 20% polyethylene glycol 3000, 0.2 M calcium acetate, and 0.1 M Tris-HCl (pH 7.0) (Figure S1b of the Supporting Information), and the other was in droplet B consisting of 20% polyethylene glycol 3350, 0.2 M sodium acetate, and 0.1 M Bis-Tris propane (pH 7.5). Within 3 weeks, both crystals in these drops grew at 20 °C to a size of >0.1 mm. Diffraction images were acquired at up to 2.20 Å resolution for the crystal (wild-type *Pedobacter* Hep III) in droplet A and 2.40 Å resolution for the crystal (the I29V/L657S mutant) in droplet B after cyoprotection. The results of X-ray data collection are listed in Table 1.

The refined model for *Pedobacter* Hep III comprised 637 residues and 131 water molecules for a protein molecule in an asymmetric unit. All amino acid residues (Ile-29-//-Pro-659-Leu-660-Glu-661-His-662-His-663-His-664-His-665), except for the N-terminal residues (Met-1-Gln-25-Ser-26-Ser-27-Ser-28) and a portion of the C-terminal His-tagged sequence (His-666-His-667), could be assigned well in the $2F_o - F_c$ map.

The final overall *R* factor for the refined model was 0.195 at up to 2.20 Å resolution. The final free *R* factor calculated using 5% of randomly selected data was 0.244. The final root-mean-square deviations (rmsds) from the standard geometry were 0.0050 Å for bond lengths and 0.995° for bond angles. On the basis of the results of Ramachandran plot analysis for which the stereochemical correctness of the backbone structure was indicated by the φ and ψ torsion angles,[37] most of the non-glycine residues were within the most favored regions, and the other residues were in additional and generously allowed regions. The structure of the I29V/L657S mutant crystallized in droplet B was determined by molecular replacement using refined wild-type coordinates as an initial model, although the mutant was also crystallized in droplet A. Refinement statistics are listed in Table 1. Although the compositions of droplets A and B mutually differ, properties of crystals formed in both droplets are identical. The structure of I29V/L657S was also essentially identical with that of wild-type *Pedobacter* Hep III other than the interdomain relationship described below.

Overall Structure. The overall structure (Figure 2a) indicated that *Pedobacter* Hep III was composed of two globular domains (N- and C-terminal domains) that formed α- and β-structures, respectively. The N-terminal domain comprised 350 residues from Ile-29 to Ala-378 and one metal ion and was predominantly composed of 15 α-helices (HA0–HA3, HA3′, HA4, HA4′, and HA5–HA12), 12 of which formed an α/α-barrel structure (Figure 2b). The C-terminal domain comprised 268 residues from Lys-392 to Pro-659 and one metal ion and consisted of one helix (HB1) and 20 β-strands (SA1–SA4, SB1–SB4, SC1–SC9, and SD1–SD3) arranged in four antiparallel β-sheets [sheets A–D (Figure 2c)]. A peptide linker comprising 13 residues from Thr-379 to Ser-391 connected the N- and C-terminal domains.

Two metal ions were included in the N- and C-terminal domains (Figure 2a). Because droplet A included calcium acetate, these metal ions were probably calcium ions. Although EDTA barely inhibited the enzyme activity of *Pedobacter* Hep III in our assay, calcium ions are known to be required for its activity.[38] Two calcium ion-binding sites (Leu-390–Gly-405 and Arg-576–Asn-591) were postulated for the *Pedobacter* Hep III molecule based on its primary structure.[38] However, these putative sites did not correspond to calcium-binding sites in the crystal structure. The four atoms (ND1 of His-241, OE1 of Glu-245, and two oxygen atoms of water molecules) in the N-terminal domain were coordinated to a calcium ion. The distance between this calcium ion and the oxygen atoms ranged from 2.1 to 2.7 Å (average of 2.3 Å). On the other hand, six atoms (OE1 of Gln-426, OD1 of Asp-444, NE2 of His-469, and three oxygen atoms of water molecules) were coordinated to a calcium ion bound to the C-terminal domain, and the coordination geometry comprised a distorted octahedron. The distance between this calcium ion and the oxygen atoms ranged from 2.1 to 2.4 Å (average of 2.2 Å).

We searched for structural homologues of *Pedobacter* Hep III in the PDB using *DALI*.[39] Several proteins with N-terminal α/α-barrels and C-terminal antiparallel β-sheets as a basic scaffold were found to be structurally homologous with *Pedobacter* Hep III (Table S2 of the Supporting Information). The overall structure of *Pedobacter* Hep III was most similar to the recently determined structure of family PL-12 Hep III from *B. thetaiotaomicron* (PDB entry 4fnv; Z = 50.3)[23] with an rmsd of 4.6 Å for 659 C^{α} atoms, although the level of sequence identity between these two was not very high (28%). *Pedobacter* Hep III was also structurally similar to other polysaccharide lyases, such as family PL-15 alginate lyase Atu3025[40] from *Agrobacterium tumefaciens* (PDB entry 3a0o; Z = 25.0), family PL-21 *Pedobacter* Hep II[22] (PDB entry 3e80; Z = 24.2), and family PL-8 chondroitin AC lyase from *Arthrobacter aurescens* (PDB entry 1rw9; Z = 21.8). A superimposition of the crystal structures of *Pedobacter* and *Bacteroides* Hep IIIs is shown in Figure 3a. The distance between the two domains of *Pedobacter* Hep III was greater than that for *Bacteroides* Hep III, which indicated that *Pedobacter* Hep III exhibited an open form with two domains mutually separated.

A large number of polysaccharide lyases with α/α-barrels were categorized into the superfamily of chondroitin AC/alginate lyase in an "α/α toroid" fold in the SCOP database (http://scop.mrc-lmb.cam.ac.uk/scop/). *Pedobacter* Hep III will be structurally classified into this "α/α toroid" fold in the SCOP database.

Active Site. The catalytic reactions of polysaccharide lyases can be divided into three steps as follows.[41] (1) Positively charged residues (residue A) stabilize or neutralize the negative charge on the C-6 carboxylate anion. (2) A general base catalyst (residue B) abstracts the proton from C-5 of the uronic acid residue. (3) A general acid catalyst (residue C) donates a proton to the glycoside bond to be cleaved. To assess the enzyme catalytic mechanism, we made every effort to prepare enzyme crystals in complexes with heparin oligosaccharides, although this failed.

Because *Pedobacter* Hep III was structurally similar to *Pedobacter* Hep II complexed with heparin tetrasaccharide (PDB entry 3e7j),[42] the active site in *Pedobacter* Hep III was analyzed through superimposition of *Pedobacter* Hep III on *Pedobacter* Hep II/tetrasaccharide. In the case of *Pedobacter* Hep II, the tetrasaccharide is bound to the cleft that is formed

between the N-terminus and the central subdomains, which correspond to the N- and C-terminal domains of *Pedobacter* Hep III, respectively.[42] Because of the open form of *Pedobacter* Hep III, two N- and C-terminal domains were analyzed separately. The N-terminal domain of *Pedobacter* Hep III was superimposed on the N-terminal subdomain of *Pedobacter* Hep II/tetrasaccharide (Figure 3b), and the C-terminal domain of *Pedobacter* Hep III was superimposed on the central subdomain of *Pedobacter* Hep II/tetrasaccharide (Figure 3c).

On the basis of the complex structure of *Pedobacter* Hep II/tetrasaccharide, the following reaction mechanism of *Pedobacter* Hep II catalysis was proposed.[42] His-406 functions as a neutralizer (residue A) for the substrate carboxyl group, and Tyr-257 successively functions as a general base and acid (residues B and C) for GlcUA-containing heparin. His-202 is also considered to be crucial for enzyme catalysis as a general base (residue B) for a substrate that contains IdoA.

Structural comparisons indicated that His-202, Tyr-257, and His-406 of *Pedobacter* Hep II corresponded to His-241, Tyr-294, and His-424, respectively, of *Pedobacter* Hep III. In the case of *Pedobacter* Hep III, His-241 appeared to be slightly farther from the tetrasaccharide (Figure 3c). This was due to the open form of *Pedobacter* Hep III, and His-241 was located near the tetrasaccharide in the possible closed conformation, as seen in the superimposition of both N-terminal domains of *Pedobacter* Hep III and *Pedobacter* Hep II/tetrasaccharide (Figure 3b).

Three *Pedobacter* Hep III mutants, H241A, Y294F, and H424A, were constructed by site-directed mutagenesis, purified to homogeneity (Figure S1a of the Supporting Information), and used for enzyme assays. The specific activities of H241A, Y294F, and H424A toward heparan sulfate are listed in Table 2.

Table 2. Specific Activity of *Pedobacter* Hep III Wild-Type and Mutant Enzymes toward Heparan Sulfate

protein	specific activity (units/mg of protein)[a]	relative activity (%)
wild-type	22.6 ± 2.90	100
I29V/L657S	9.64 ± 1.51	42.7
E237A	9.23 ± 2.34	40.8
Q238A	20.0 ± 3.20	88.5
N240A	0.693 ± 0.212	3.07
H241A	6.71 ± 1.43	29.7
Y294F	0.638 ± 0.146	2.82
W350A	6.14 ± 1.08	27.2
F423A	9.59 ± 0.960	42.4
H424A	0.0699 ± 0.0183	0.309
Y450F	1.26 ± 0.123	5.58
Y590F	1.75 ± 0.404	7.74

[a]Each value represents the average of triplicate individual experiments (mean ± the standard deviation).

These mutants had significantly reduced enzyme activity compared with that of the wild-type enzyme. In particular, Tyr-294 and His-424 were suggested to be crucial for enzyme activity as with *Pedobacter* Hep II. The mutation at His-241 has also been demonstrated to reduce the turnover number (k_{cat}) of the enzyme.[20]

Other than putative catalytic residues (Tyr-294 and His-424), seven residues (Glu-237, Gln-238, Asn-240, Trp-350, Phe-423, Tyr-450, and Tyr-590) located at the active site (Figure 3b,c) were substituted with an Ala or Phe residue by site-directed mutagenesis. Seven mutants (E237A, Q238A, N240A, W350A, F423A, Y450F, and Y590F) were purified to homogeneity (Figure S1a of the Supporting Information) and used for enzyme assays. The specific activities of these mutants toward heparan sulfate are also listed in Table 2. Among these mutants, N240A had significantly reduced enzyme activity, which suggested that Asn-240 in conjunction with Tyr-294 and His-424 was involved in enzyme activity as a stabilizer or catalyst (residue A, B, or C). In fact, these Asn, Tyr, and His residues were conserved in all three heparan sulfate lyases from *P. heparinus*, *B. thetaiotaomicron*, and *Bacteroides stercoris* that have been well characterized.[9,23,43] The importance of these residues has also been reported for *B. thetaiotaomicron* Hep III.[23]

Two histidine residues, His-295 and His-510, are suggested to be crucial for the enzyme activity of *Pedobacter* Hep III by site-directed mutagenesis.[20] His-295 constituted the active site in the crystal structure (Figure 3b), although His-510 was situated far from the active cleft. The crystal structure of this enzyme in complex with heparin-derived saccharides will be needed to elucidate mechanisms of *Pedobacter* Hep III for its catalytic reaction and substrate recognition.

Interactions between *Pedobacter* Hep III and Heparin Oligosaccharides. To analyze its substrate binding, *Pedobacter* Hep III was subjected to differential scanning fluorimetry based on changes in protein stability by ligand binding in the presence of a dye, SYPRO Orange. Various saccharides were used as the ligand at concentrations ranging from 0 to 1 mM. The fluorescence of the dye bound to denatured proteins was measured during heat treatment from 25 to 95 °C. The fluorescence profile of *Pedobacter* Hep III in the presence of heparin oligosaccharides, particularly tetrasaccharides, significantly shifted to a lower temperature as compared with that in the absence of saccharides (Figure 4). Melting temperatures, T_m, of *Pedobacter* Hep III in the absence and presence of saccharides were determined as the midpoints of the increases in the fluorescence profiles (Table 3). Among various saccharides, heparin di- and tetrasaccharides showed effects by lowering the T_m. The T_m shifted to a lower temperature with an increased concentration of added heparin tetrasaccharide. Even a small amount of tetrasacharide at a concentration of <0.01 mM significantly reduced the T_m. This suggested that *Pedobacter* Hep III had an affinity for heparin oligosaccharides and that ligand-bound *Pedobacter* Hep III was thermally less stable than the ligand-free protein. The difficulty with preparing a ligand-bound enzyme crystal may have been due to the instability of the structure of this complex.

The shift in T_m suggested a conformational change in *Pedobacter* Hep III through binding to heparin oligosaccharides. Because the N240A and H241A mutants exhibited lower enzyme activity, Asn-240 and His-241 were considered to be involved in substrate binding by conversion of the open form to the closed form (Figure 3b,c). This conversion was supported by another crystal structure of the enzymatically active *Pedobacter* Hep III double mutant (I29V/L657S) in the relatively closed form (Figure S2 of the Supporting Information). Although the properties of the mutant crystal formed in droplet B were comparable with those of the wild-type enzyme (Table 1), the N- and C-terminal domains of the mutant were close to each other. On the basis of the results of differential scanning fluorimetry and site-directed mutagenesis, *Pedobacter* Hep III is suggested to exhibit domain dynamics by substrate binding and product release.

dx.doi.org/10.1021/bi4012463 | *Biochemistry* 2014, 53, 777−786

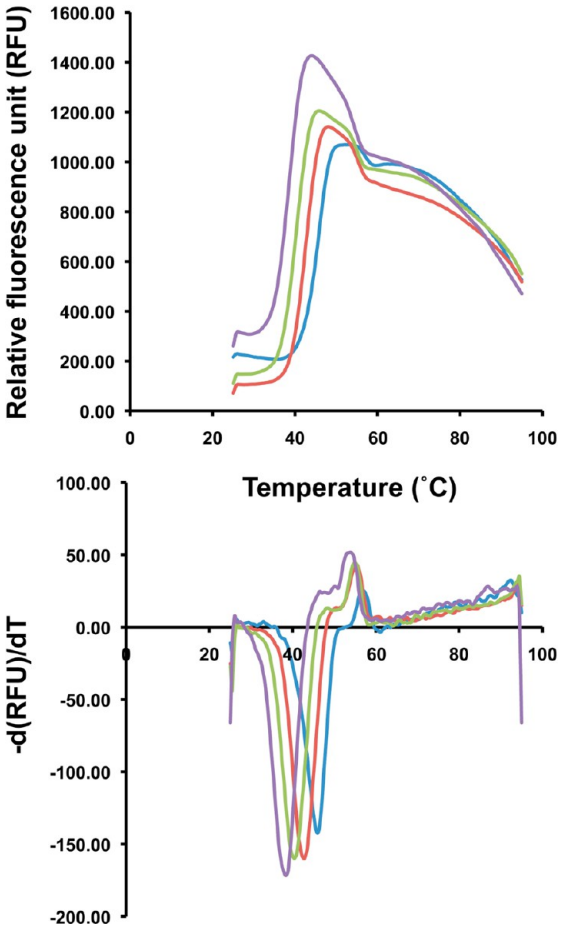

Figure 4. Ligand binding analysis by differential scanning fluorimetry. The top panel shows the fluorescence profile of *Pedobacter* Hep III with heparin tetrasaccharide (blue, 0 mM; brown, 0.01 mM; green, 0.1 mM; purple, 1 mM). The tetrasaccharide purchased from Iduron was obtained mainly from the disaccharide units of IdoA and GlcN with sulfate groups at C2 and N positions, respectively, and the nonreducing uronate residue has a C4−C5 double bond. The bottom panel shows a negative derivative curve plot obtained from the fluorescence profile.

As shown in Figure 1b, positively charged clusters derived from basic residues (Lys-83, Lys-111, Arg-140, and Arg-188) are located at the substrate-binding cleft of *Pedobacter* Hep III. All of them lie at the N-terminal side of the cleft, and the C-terminal side includes no basic residues, suggesting that the acidic substrate of heparan sulfate first binds to *Pedobacter* Hep III at the N-terminal side, followed by a conformational change to the closed form. The three positively charged residues, Lys-111, Arg-140, and Arg-188, of *Pedobacter* Hep III correspond to Lys-101, Arg-131, and Arg-195, respectively, of *B. stercoris* Hep III, although these basic residues are hardly conserved in *B. thetaiotaomicron* Hep III and there is a significant difference in electrostatic features on the overall molecular surface between *Pedobacter* and *Bacteroides* Hep IIIs (Figure 1b). Compared with the surface structure of *Pedobacter* Hep III, *Pedobacter* Hep II preferring sulfated substrate shows additional positive charge at the C-terminal side of the cleft. The difference in molecular surface charge may be a structural determinant for the substrate specificity of *Pedobacter* Hep III.

In conclusion, *Pedobacter* Hep III comprised an N-terminal α/α-barrel domain and a C-terminal antiparallel β-sheet domain, both of which were flexible by hinge bending. Through its binding to a substrate, this enzyme seems to be converted to the closed form with access to its two domains. The active site in *Pedobacter* Hep III is probably located in the deep cleft at the interface between these two domains.

Table 3. Temperature Denaturation Transitions for *Pedobacter* Hep III

ligand	concentration (mM)	T_m (°C)
none		45.44
heparin tetrasaccharide	0.00001	45.44
	0.00005	45.01
	0.0001	44.79
	0.0005	43.93
	0.001	43.72
	0.005	42.64
	0.01	42.21
	0.05	42.21
	0.1	40.48
	0.5	40.06
	1	39.40
heparin disaccharide	0.01	44.15
	0.1	43.93
	0.5	43.72
	1	43.50
gellan tetrasaccharide	0.01	45.83
	0.1	45.19
	1	44.97
GlcNAc	0.01	44.53
	0.1	44.31
	1	44.31

■ ASSOCIATED CONTENT

Ⓢ Supporting Information

Supplementary data. This material is available free of charge via the Internet at http://pubs.acs.org.

■ AUTHOR INFORMATION

Corresponding Author

*Laboratory of Basic and Applied Molecular Biotechnology, Graduate School of Agriculture, Kyoto University, Uji, Kyoto 611-0011, Japan. E-mail: whasimot@kais.kyoto-u.ac.jp. Telephone: +81-774-38-3756. Fax: +81-774-38-3767.

Present Address

§K.M.: Faculty of Science and Engineering, Setsunan University, Neyagawa, Japan.

Funding

This work was supported in part by Grants-in-Aid from the Japan Society for the Promotion of Science (K.M. and W.H.) and by the Targeted Proteins Research Program (W.H.) from the Ministry of Education, Culture, Sports, Science, and Technology (MEXT) of Japan.

Notes

The authors declare no competing financial interests.

This structural study was first presented at the Annual Meeting of the Japan Society for Bioscience, Biotechnology, and Agrochemistry, held in Kyoto, Japan, on March 25, 2012.

■ ACKNOWLEDGMENTS

We thank Drs. S. Baba and N. Mizuno of the Japan Synchrotron Radiation Research Institute (JASRI) for their

kind help with data collection. Diffraction data for crystals were acquired at the BL-38B1 station of SPring-8 (Hyogo, Japan) with the approval of JASRI (Projects 2011B2055, 2012A1317, 2012B1265, and 2013A1106). We also thank Ms. Ai Matsunami for her excellent technical assistance.

■ ABBREVIATIONS

GlcUA, D-glucuronic acid; GalNAc, *N*-acetyl-D-galactosamine; GlcNAc, *N*-acetyl-D-glucosamine; IdoA, L-iduronic acid; Hep I, heparin lyase I of *P. heparinus*; Hep II, heparin lyase II of *P. heparinus*; Hep III, heparin lyase III of *P. heparinus* or *B. thetaiotaomicron*; PCR, polymerase chain reaction; LB, Luria-Bertani; SDS−PAGE, sodium dodecyl sulfate−polyacrylamide gel electrophoresis; PDB, Protein Data Bank; RFU, relative fluorescence unit; rmsd, root-mean-square deviation; T_m, melting temperature.

■ REFERENCES

(1) Gandhi, N. S., and Mancera, R. L. (2008) The structure of glycosaminoglycans and their interactions with proteins. *Chem. Biol. Drug Des. 72*, 455−482.
(2) Hascall, V., and Esko, J. D. (2009) *Essentials of Glycobiology*, 2nd ed., Cold Spring Harbor Laboratory Press, Plainview, NY.
(3) Lindahl, U., and Höök, M. (1978) Glycosaminoglycans and their binding to biological macromolecules. *Annu. Rev. Biochem. 47*, 385−417.
(4) Jedrzejas, M. J. (2007) Unveiling molecular mechanisms of bacterial surface proteins: *Streptococcus pneumoniae* as a model organism for structural studies. *Cell. Mol. Life Sci. 64*, 2799−2822.
(5) Ernst, S., Langer, R., Cooney, C. L., and Sasisekharan, R. (1995) Enzymatic degradation of glycosaminoglycans. *Crit. Rev. Biochem. Mol. Biol. 30*, 387−444.
(6) Ponnuraj, K., and Jedrzejas, M. J. (2000) Mechanism of hyaluronan binding and degradation: Structure of *Streptococcus pneumoniae* hyaluronate lyase in complex with hyaluronic acid disaccharide at 1.7 Å resolution. *J. Mol. Biol. 299*, 885−895.
(7) Payza, A. N., and Korn, E. D. (1956) Bacterial degradation of heparin. *Nature 177*, 88−89.
(8) Galliher, P. M., Cooney, C. L., Langer, R., and Linhardt, R. J. (1981) Heparinase production by *Flavobacterium heparinum*. *Appl. Environ. Microbiol. 41*, 360−365.
(9) Lohse, D. L., and Linhardt, R. J. (1992) Purification and characterization of heparin lyases from *Flavobacterium heparinum*. *J. Biol. Chem. 267*, 24347−24355.
(10) Cantarel, B. L., Coutinho, P. M., Rancurel, C., Bernard, T., Lombard, V., and Henrissat, B. (2009) The Carbohydrate-Active EnZymes database (CAZy): An expert resource for glycogenomics. *Nucleic Acids Res. 37*, D233−D238.
(11) Huang, W., Matte, A., Li, Y., Kim, Y. S., Linhardt, R. J., Su, H., and Cygler, M. (1999) Crystal structure of chondroitinase B from *Flavobacterium heparinum* and its complex with a disaccharide product at 1.7 Å resolution. *J. Mol. Biol. 294*, 1257−1269.
(12) Féthière, J., Eggimann, B., and Cygler, M. (1999) Crystal structure of chondroitin AC lyase, a representative of a family of glycosaminoglycan degrading enzymes. *J. Mol. Biol. 288*, 635−647.
(13) Sasisekharan, R., Leckband, D., Godavarti, R., Venkataraman, G., Cooney, C. L., and Langer, R. (1995) Heparinase I from *Flavobacterium heparinum*: The role of the cysteine residue in catalysis as probed by chemical modification and site-directed mutagenesis. *Biochemistry 34*, 14441−14448.
(14) Godavarti, R., Cooney, C. L., Langer, R., and Sasisekharan, R. (1996) Heparinase I from *Flavobacterium heparinum*. Identification of a critical histidine residue essential for catalysis as probed by chemical modification and site-directed mutagenesis. *Biochemistry 35*, 6846−6852.
(15) Godavarti, R., and Sasisekharan, R. (1998) Heparinase I from *Flavobacterium heparinum*. Role of positive charge in enzymatic activity. *J. Biol. Chem. 273*, 248−255.
(16) Shriver, Z., Hu, Y., Pojasek, K., and Sasisekharan, R. (1998) Heparinase II from *Flavobacterium heparinum*. Role of cysteine in enzymatic activity as probed by chemical modification and site-directed mutagenesis. *J. Biol. Chem. 273*, 22904−22912.
(17) Shriver, Z., Hu, Y., and Sasisekharan, R. (1998) Heparinase II from *Flavobacterium heparinum*. Role of histidine residues in enzymatic activity as probed by chemical modification and site-directed mutagenesis. *J. Biol. Chem. 273*, 10160−10167.
(18) Su, H., Blain, F., Musil, R. A., Zimmermann, J. J., Gu, K., and Bennett, D. C. (1996) Isolation and expression in *Escherichia coli* of *hepB* and *hepC*, genes coding for the glycosaminoglycan-degrading enzymes heparinase II and heparinase III, respectively, from *Flavobacterium heparinum*. *Appl. Environ. Microbiol. 62*, 2723−2734.
(19) Godavarti, R., Davis, M., Venkataraman, G., Cooney, C. L., Langer, R., and Sasisekharan, R. (1996) Heparinase III from *Flavobacterium heparinum*: Cloning and recombinant expression in *Escherichia coli*. *Biochem. Biophys. Res. Commun. 225*, 751−758.
(20) Pojasek, K., Shriver, Z., Hu, Y., and Sasisekharan, R. (2000) Histidine 295 and histidine 510 are crucial for the enzymatic degradation of heparan sulfate by heparinase III. *Biochemistry 39*, 4012−4019.
(21) Han, Y. H., Garron, M. L., Kim, H. Y., Kim, W. S., Zhang, Z., Ryu, K. S., Shaya, D., Xiao, Z., Cheong, C., Kim, Y. S., Linhardt, R. J., Jeon, Y. H., and Cygler, M. (2009) Structural snapshots of heparin depolymerization by heparin lyase I. *J. Biol. Chem. 284*, 34019−34027.
(22) Shaya, D., Tocilj, A., Li, Y., Myette, J., Venkataraman, G., Sasisekharan, R., and Cygler, M. (2006) Crystal structure of heparinase II from *Pedobacter heparinus* and its complex with a disaccharide product. *J. Biol. Chem. 281*, 15525−15535.
(23) Dong, W., Lu, W., McKeehan, W. L., Luo, Y., and Ye, S. (2012) Structural basis of heparan sulfate-specific degradation by heparinase III. *Protein Cell 3*, 950−961.
(24) Sambrook, J., Fritsch, E. F., and Maniatis, T. (1989) *Molecular cloning: A laboratory manual*, Cold Spring Harbor Laboratory Press, Plainview, NY.
(25) Doublié, S., and Carter, C. W. J. (1992) *Crystallographic Nucleic Acids Proteins*, Oxford University Press, Oxford, U.K.
(26) Laemmli, U. K. (1970) Cleavage of structural proteins during the assembly of the head of bacteriophage T4. *Nature 227*, 680−685.
(27) Otwinowski, Z., and Minor, W. (1997) Processing of X-ray diffraction data collected in oscillation mode. *Methods Enzymol. 276*, 307−326.
(28) Adams, P. D., Afonine, P. V., Bunkóczi, G., Chen, V. B., Davis, I. W., Echols, N., Headd, J. J., Hung, L. W., Kapral, G. J., Grosse-Kunstleve, R. W., McCoy, A. J., Moriarty, N. W., Oeffner, R., Read, R. J., Richardson, D. C., Richardson, J. S., Terwilliger, T. C., and Zwart, P. H. (2010) PHENIX: A comprehensive Python-based system for macromolecular structure solution. *Acta Crystallogr. D66*, 213−221.
(29) Emsley, P., and Cowtan, K. (2004) Coot: Model-building tools for molecular graphics. *Acta Crystallogr. D60*, 2126−2132.
(30) Murshudov, G. N., Vagin, A. A., and Dodson, E. J. (1997) Refinement of macromolecular structures by the maximum-likelihood method. *Acta Crystallogr. D53*, 240−255.
(31) Lovell, S. C., Davis, I. W., Arendall, W. B., III, de Bakker, P. I. W., Word, J. M., Prisant, M. G., Richardson, J. S., and Richardson, D. C. (2003) Structure validation by Cα geometry: Φ, Ψ and Cβ deviation. *Proteins 50*, 437−450.
(32) DeLano, W. L. (2004) *The PyMOL molecular graphics system*, DeLano Scientific LLC, San Carlos, CA.
(33) Berman, H. M., Westbrook, J., Feng, Z., Gilliland, G., Bhat, T. N., Weissig, H., Shindyalov, I. N., and Bourne, P. E. (2000) The protein data bank. *Nucleic Acids Res. 28*, 235−242.
(34) Sanger, F., Nicklen, S., and Coulson, A. R. (1977) DNA sequencing with chain-terminating inhibitors. *Proc. Natl. Acad. Sci. U.S.A. 74*, 5463−5467.

(35) Niesen, F. H., Berglund, H., and Vedadi, M. (2007) The use of differential scanning fluorimetry to detect ligand interactions that promote protein stability. *Nat. Protoc. 2*, 2212−2221.
(36) Hashimoto, W., Maesaka, K., Sato, N., Kimura, S., Yamamoto, K., Kumagai, H., and Murata, K. (1997) Microbial system for polysaccharide depolymerization: Enzymatic route for gellan depolymerization by *Bacillus* sp. GL1. *Arch. Biochem. Biophys. 339*, 17−23.
(37) Ramachandran, G. N., and Sasisekharan, V. (1968) Conformations of polypeptides and proteins. *Adv. Protein Chem. 23*, 283−438.
(38) Godavarti, R., and Sasisekharan, R. (1996) A comparative analysis of the primary sequences and characteristics of heparinases I, II, and III from *Flavobacterium heparinum*. *Biochem. Biophys. Res. Commun. 229*, 770−777.
(39) Holm, L., and Sander, C. (1993) Protein structure comparison by alignment of distance matrices. *J. Mol. Biol. 233*, 123−138.
(40) Ochiai, A., Yamasaki, M., Mikami, B., Hashimoto, W., and Murata, K. (2010) Crystal structure of exotype alginate lyase Atu3025 from *Agrobacterium tumefaciens*. *J. Biol. Chem. 285*, 24519−24528.
(41) Garron, M. L., and Cygler, M. (2010) Structural and mechanistic classification of uronic acid-containing polysaccharide lyases. *Glycobiology 20*, 1547−1573.
(42) Shaya, D., Zhao, W., Garron, M. L., Xiao, Z., Cui, Q., Zhang, Z., Sulea, T., Linhardt, R. J., and Cygler, M. (2010) Catalytic mechanism of heparinase II investigated by site-directed mutagenesis and the crystal structure with its substrate. *J. Biol. Chem. 285*, 20051−20061.
(43) Hyun, Y. J., Lee, J. H., and Kim, D. H. (2010) Cloning, overexpression, and characterization of recombinant heparinase III from *Bacteroides stercoris* HJ-15. *Appl. Microbiol. Biotechnol. 86*, 879−890.